Journal of Materials Chemistry

Cite this: J. Mater. Chem., 2011, 21, 15975

www.rsc.org/materials

PAPER

Helical columnar liquid crystals based on dendritic peptides substituted perylene bisimides†

Baoxiang Gao,*[ab] Defang Xia,[a] Licui Zhang,[a] Qianqian Bai,[a] Libin Bai,[ab] Tao Yang[ab] and Xinwu Ba[ab]

Received 7th July 2011, Accepted 4th August 2011
DOI: 10.1039/c1jm13144c

New columnar liquid crystals based on perylene bisimides (PBIs) were synthesized by introducing dendritic peptides onto the two ends of the imide. The self-assembly behaviour of PBIs in solution and in film was investigated through temperature-dependent and solvent-dependent ultraviolet-visible absorption spectroscopy. The mesomorphic behaviour was studied by polarizing optical microscopy, differential scanning calorimetry, small-angle X-ray diffraction and temperature-dependent Fourier transform infrared spectroscopy. Ordered columnar mesophases were observed for PBIs at room temperature. Circular dichroism studies demonstrate that these materials exhibit supramolecular optical activity in the liquid crystalline state, which is attributed to helical columnar organization. The hydrogen bonds at the periphery of PBIs result in the ordered columnar mesophases structure with small inter-disk distances of 3.4 Å

Introduction

The unique structural and electronic properties of columnar liquid crystal materials have attracted considerable attention because of their potential applications in devices, such as field-effect transistors, electroluminescent displays, and photovoltaic cells.[1] The cofacially π-stacked structures of the disk-like aromatics in the columnar liquid crystal phases are widely recognized as an efficient pathway to promoting one-dimensional electrical conduction.[2,3] In particular, various examples of columnar liquid crystal molecules, such as triphenylenes,[4] *m*-phenylene ethynylene oligomers,[5] hexabenzocoronenes,[6] triindoles,[7] and phthalocyanines,[8] form π stacks with helical superstructures that exhibit increased charge-carrier mobilities as a result of the higher molecular order. Most semiconducting discotics are good hole-transporting materials (p-type), whereas only a limited number of good electron-transporting materials (n-type) were reported.[9] Perylene-3,4:9,10-tetracarboxydiimides (PBIs), have attracted interest as electron-transporting materials with high electron mobilities.[10] However, most of the thermotropic liquid crystalline PBI derivatives reported in literature are not columnar liquid crystals.[11] Columnar liquid crystal PBI derivatives are difficult to design and synthesize because of their low symmetry. The pioneering work of Würthner and co-workers involved columnar hexagonal PBIs with tridodecylphenyl substituents, as well as perylene bay substitution.[12] Jin and co-workers reported crystalline π stacks in the highly ordered columnar PBIs smectic phase.[13] Recently, Thelakkat reported on columnar liquid crystalline PBIs with swallow-tail side-chains.[14] Despite the great interest in columnar liquid crystals with helical superstructures, only one PBI derivative with chiral side chains exhibits chiral columnar liquid crystalline structure.[15]

Dendrimers and dendrons prove to be particularly versatile candidates as novel and original scaffoldings for the synthesis of new liquid crystalline materials.[16] These tapered dendritic molecules aggregate into infinite supramolecular columns with a polar interior, these columns, which are separated from each other by the aliphatic medium, self-organize into rectangular or hexagonal lattices.[17] Furthermore, Kato and co-workers showed that dendritic oligopeptides are useful building blocks for the synthesis of supramolecular chiral columnar liquid crystals.[18]

In the present study, novel dendritic peptides substituted perylene bisimides (DPPBIs) capable of forming liquid crystalline assembly are reported. In particular, DPPBIs can form an ordered hexagonal columnar liquid crystals over a wide temperature range, including room temperature. The chiral peptides induce PBIs to form a helical superstructure. The addition of hydrogen-bonding motifs to the periphery of PBIs is carried out in order to study the effect of hydrogen bonding on the already pronounced columnar stacking.

Experimental

General information

Perylenetetracarboxylic acid dianhydride PTCDA was purchased fromLiaoning Liangang Pigment and Dyestuff

[a]College of Chemistry and Environmental Science, Hebei University, Baoding, 071002, P. R. China. E-mail: bxgao@hbu.edu.cn; Fax: +86 3125079317
[b]Key Laboratory of Medicinal Chemistry and Molecular Diagnosis, Ministry of Education, Hebei University, Baoding, 071002, P. R. China
† Electronic supplementary information (ESI) available. See DOI: 10.1039/c1jm13144c

Chmeicals Co. Ltd. L-Aspartic acid and *N*-carbobenzyloxy-L-aspartic acids were purchased from Yangzhou Baosheng Bio-Chemical Co. Ltd. *N*-(3-Dimethylaminopropyl)-*N*′-ethyl-carbodiimide hydrochloride (EDCI), 4-dimethylaminopyridine and 1-hydroxybenzotrizole were purchased from Shanghai Medpep Co. Ltd. Imidazole, and solvents were purchased from Sinopharm Chemical Reagent Co.Ltd, and used without any further purification. Solvents used for precipitation and column chromatography were distilled under normal atmosphere. The ^{1}H NMR spectra were recorded at 20 °C on a 400 or 600 MHz NMR spectrometer (Bruker). Chemical shifts are reported in ppm at room temperature using $CDCl_3$ as the solvent and tetramethylsilane as an internal standard unless indicated otherwise. Abbreviations used for splitting patterns are s = singlet, d = doublet, t = triplet, qui = quintet, m = multiplet. Mass spectra were carried out using MALDI-TOF/TOF matrix assisted laser desorption ionization mass spectrometry with autoflexIII smartbeam (Bruker Daltonics Inc). FTIR-spectra were recorded with a Varian 640-IR in the range of 400–4000 cm^{-1}. UV/Vis spectra were recorded with a Shimadzu WV-2550 spectrophotometer. Differential scanning calorimetry (DSC) was carried out with a Perkin Elmer differential scanning calorimeter (DSC7) with heating and cooling rates of 10 K min^{-1}. Phase transitions were also examined by a polarization optical microscop (POM) Olympus BX51 with a T95-PE temperature-controlled THMS-600 hot stage. X-ray diffraction measurements were performed on a D8 Advance (Bruker AXS Inc.) with Cu-Kα1: 1.54051 Å. Circular dichroism spectra were recorded on a Jasco J-810 spectropolarimeter, and the date of every sample is the average of there times scan.

Synthesis and characterization of PBIs

Compound 2. 2.67 g of *N*-carbobenzyloxyl-aspartic acid (10.0 mmol) was dissolved in 60 mL of DCM, 4.79 g EDCI (25.0 mmol) was added, and the mixture was stirred at 0 °C for 30 min. 3.72 g 1-Dodecanol (20.0 mmol) and 0.25 g DMAP (2.0 mmol) were added and the mixture stirred at room temperature for 24 h. Solvent was removed by rotary evaporation. The residue was purified by column chromatography on silica gel with methylene chloride as the eluent to afford compound **2** as a white solid (5.32 g, 88%). ^{1}H-NMR (300 Hz, $CDCl_3$): δ (ppm) 7.36–7.30(m, 5H), 5.76 (d, J = 8.5 Hz, 1H), 5.14 (s, 2H), 4.63 (dd, J = 8.7 Hz, 1H), 4.13(d, J = 3.6 Hz 2H), 4.06 (t, J = 6.8 Hz, 2H), 3.04–2.82 (m, 2H), 1.63–1.57 (m, 4H), 1.30–1.26 (m, 36H), 0.88 (t, J = 7.1 Hz, 6H). ^{13}C-NMR (150 MHz, $CDCl_3$): 170.83, 170.72, 155.96, 136.23, 128.52, 128.17, 128.06, 67.04, 66.01, 65.25, 50.49, 36.71, 31.92, 29.64, 29.59, 29.52, 29.36, 29.24, 29.22, 28.52, 28.45, 25.85, 25.79, 22.69, 14.11. Anal. calcd for $C_{36}H_{61}NO_6$: C, 71.60; H, 10.18; N, 2.32. found: C, 71.83; H, 10.02; N, 2.01. *m*/*z* [MALDI-TOF]: 604.7 (MH^+).

Compound 3. 4.86 g of compound **2** (8.0 mmol) dissolved in 110 mL ethanol and 0.50 g of 10% Pd/C catalyst was added. The mixture was hydrogenated overnight in a Parr shaker at 2 psi H_2. The reaction mixture was then filtered and the solvent was removed under reduced pressure to give a white solid. The crude product was purified by column chromatography on silica gel with methylene chloride: ethanol (100 : 1) as an eluent to afford **3** as a white solid (3.13 g, 85%).^{1}H-NMR (400 Hz, $CDCl_3$): δ (ppm) 4.14–4.07 (m, 2H), 3.81–3.79(m, 1H), 2.81–2.67 (m, 2 H), 1.63–1.60 (m, 4H), 1.30–1.26 (m, 36H), 0.88 (t, J = 7.1 Hz, 6H). ^{13}C-NMR (150 MHz, $CDCl_3$): 174.28, 171.26, 65.46, 65.00, 51.30, 39.02, 29.64, 29.57, 29.51, 29.34, 29.24, 28.55, 25.89, 25.86, 22.68, 14.09. Anal. calcd for $C_{28}H_{55}NO_4$: C, 71.59; H, 11.80; N, 2.98. found: C, 71.90; H, 11.52; N, 2.71. *m*/*z* [MALDI-TOF]: 470.4 ($M + H^+$).

Compound 6 was synthesized according to the reported procedures. Into a 50 mL Schlenk flask were charged L-aspartic acid 1.60 g (12 mmol), 3,4:9,10-perylenetetracarboxyldianhydride (PTCDA) 1.96 g (5 mmol), and imidazole (20 g). The mixture was purged with argon for 15 min before being heated at 120 °C until the reaction mixture was completely soluble in water. Subsequently, the reaction mixture was cooled to 90 °C. Deionized water was then added with the protection of argon. The dark red solution was filtered to remove the trace amount of unreacted PTCDA. The solution was then acidified with 2 M HCl aqueous solution to a pH value of 5, the precipitate was collected by suction-filtration and thoroughly washed with deionized water until the filtrate was neutral; the red solid was collected and dried at 75 °C in vacuum oven until constant weight. Analysis: compound **6** is too insoluble for NMR analysis. Anal. calcd for $C_{32}H_{18}N_2O_{12}$: C, 61.74; H, 2.91; N, 4.50. found: C, 62.05; H, 3.04; N, 4.17.

Compound SAPBI. Into a 10 ml Schlenk flask were charged compound **3** (1.03 g, 2.2 mmol), PTCDA (0.39 g, 1.0 mmol) and imidazole (8 g). The mixture was purged with argon for 15 min before being heated to 120 °C for 2 h. It was then allowed to cool to room temperature before 20 mL deionized water was added. The precipitate was collected by suction-filtration and thoroughly washed with deionized water and ethanol. The crude product was purified by column chromatography on silica gel with methylene chloride as the eluent to afford **SAPBI** as a red solid (0.67 g, 52%). ^{1}H-NMR (600 Hz, $CDCl_3$) δ (ppm) 8.72 (d, J = 7.9 Hz, 4H), 8.65 (d, J = 8.1 Hz, 4H), 6.27 (t, J = 7.2 Hz, 2 H), 4.22−4.04 (m, 8 H), 3.56 (dd, J = 6.5 Hz, 2 H), 3.06 (dd, J = 7.6 Hz, 2 H), 1.62–1.55 (m, 8H), 1.25–1.11 (m, 72H), 0.89–0.83 (m, 12H). ^{13}C NMR (150 MHz, $CDCl_3$): 170.83, 170.72, 155.96, 136.23, 128.52, 128.17, 128.06, 67.04, 66.01, 65.25, 50.49, 36.71, 31.92, 29.64, 29.59, 29.52, 29.36, 29.24, 29.22, 28.52, 28.45, 25.85, 25.79, 22.69, 14.11. Anal. calcd for $C_{80}H_{114}N_2O_{12}$: C, 74.15; H, 8.87; N, 2.16. found: C, 74.50; H, 8.56; N, 1.97. *m*/*z* [MALDI-TOF]: 1317.8 ($M + Na^+$).

Compound DPPBI. 0.31 g of compound **6** (0.5 mmol) was dissolved in 60 mL of DMF, 0.48 g EDCI(2.5 mmol) was added, and the mixture was stirred at 0 °C for 30min. 1.17 g of compound **3** (2.5 mmol) and 0.38 g HOBt (2.5 mmol) were added and the mixture stirred at room temperature for 24 h. Solvent was removed by rotary evaporation. The crude product was purified by column chromatography on silica gel with methylene chloride: ethanol (100 : 1) as an eluent to afford **DPPBI** as a red solid (1.04 g, 86%). ^{1}H-NMR (600 Hz, $CDCl_3$) δ (ppm) 8.61 (s, 4H), 8.60(s, 4H), 8.40 (br, CONH, 4H), 6.7–614 (br, 2H), 4.90 (br,4H), 4.35–3.96 (m, 16H), 3.76–3.60 (m, 4H), 3.03–2.92 (m, 8H), 1.62–1.55 (m, 16H),1.25–1.23 (m, 144H), 0.87 (m, 24H).

^{13}C-NMR (150 MHz, $CDCl_3$): 170.95, 170.88, 170.66, 170.50, 168.10, 167.98, 162.90, 134.28, 131.57, 129.04, 125.77, 123.08, 122.95, 65.99, 65.83, 65.23, 65.16, 51.56, 49.29, 49.03, 48.81, 36.67, 36.20, 36.08, 31.93, 29.66, 29.59, 29.37, 29.27, 28.57, 28.45, 25.93, 25.83, 25.80, 22.69, 14.11. Anal. calcd for $C_{144}H_{230}N_6O_{24}$: C, 71.19; H, 9.54; N, 3.46. found: C, 71.37; H, 9.26; N, 3.17. *m/z* [MALDI-TOF]: 2450.7 (M + Na^+).

Results and discussion

The chemical structures of PBIs are shown in Scheme 1. The swallow-tail amino acid-substituted perylene bisimides (**SAPBI**) were synthesized using 3,4:9,10-perylenetetracarboxyldianhydride and L-aspartic acid dodecyl ester according to the reported method.[19] For the synthesis of **DPPBI**, a two-fold condensation between 3,4:9,10-perylenetetracarboxyldianhydride and L-aspartic acid in imidazole at 120 °C for 1 h produced *N*,*N*′-di((*S*)-1,4-dicarboxy)-3,4,9,10-perylenetetracarboxyldiimide; **DPPBI** was obtained by the coupling reaction of *N*,*N*′-di((*S*)-1,4-dicarboxy)-3,4,9,10-perylenetetracarboxyldiimide and L-aspartic acid dodecyl ester in the presence of 1-ethyl-3-(3-dimethylaminopropyl) carbodiimide.

The self-assembly behaviour of PBI in solution was investigated *via* temperature-dependent and solvent-dependent ultraviolet-visible (UV-Vis) absorption spectroscopy (Fig. 1). In cyclohexane, at high temperature (80 °C), the spectrum of **SAPBI** displayed an absorption band between 400 and 550 nm, which corresponds to the S0 → S1 transition of the PBI with a well-resolved vibronic structure that can be attributed to a breathing vibration of the perylene skeleton (Fig. 1 top). Aggregation took place upon cooling, and the absorption coefficients drastically decreased, with a concomitant blue-shift of the absorption maximum, as well as a pronounced shoulder at a longer wavelength (575 nm). These spectral features are characteristic of J-aggregate PBI.[11] The aggregation is attributed to the poor solvency of cyclohexane. With a good solvent for the perylene skeleton, such as toluene and 1,4-dioxane, **SAPBI**

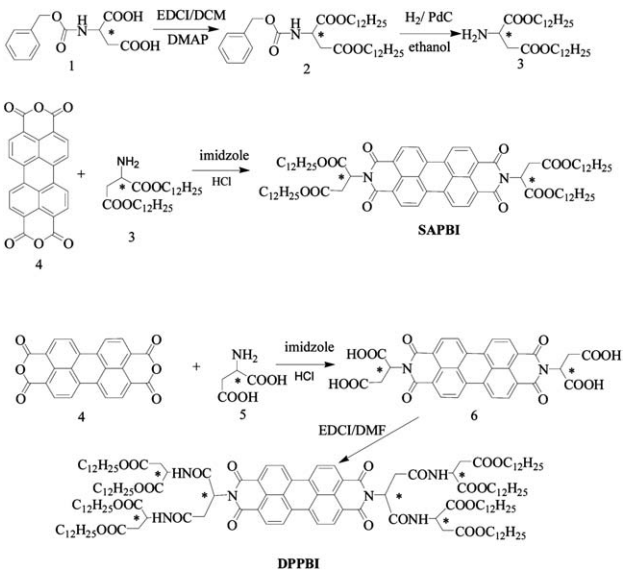

Scheme 1 The synthesis of PBIs.

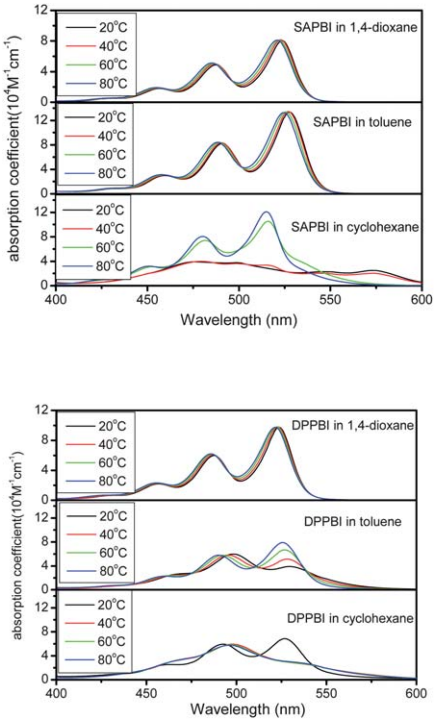

Fig. 1 Temperature dependent UV-vis absorption spectra of **SAPBI** (top) and **DPPBI** (bottom) with 1.0×10^{-4} M.

displayed a UV-Vis absorption of non-aggregated structures at a wide temperature range. **DPPBI** exhibited strong aggregation in cyclohexane at a low temperature (20 °C). When the temperature was increased from 20 to 80 °C, the aggregation of DPPBI was completely suppressed. DPPBI in toluene showed strong aggregation at a low temperature. However, aggregation did not occur in 1,4-dioxane (Fig. 1 bottom).

The self-assembly behavior of PBI in solution was further investigated *via* concentration-dependent UV-Vis and circular dichroism (CD) spectroscopies (Fig. 2). The maximum absorption of **SAPBI** appeared at 529 nm, along with two higher vibronic transitions located at 495 and 462 nm corresponding to a typical absorption of dissolved PBI molecule (Fig. 2A). The absence of a CD signal in toluene suggests that the aggregation of **SAPBI** was greatly suppressed by the bulky swallow-tail *N*-substituted groups (Fig. 2C). By contrast, the absorption bands of **DPPBI** show a well-resolved vibrational fine structure at a low concentration, which can be attributed to the vibronic transition of the PBI monomer. When the concentration was increased from 1.0×10^{-6} to 1.0×10^{-4} mol L^{-1}, the absorption coefficient of **DPPBI** dramatically decreased by 65%, and a blue shift of the absorption maximum to 491 nm was observed (Fig. 2B). The intensity reversal observed for the 0–0 and 0–1 bands indicates that the Franck–Condon factors favored the higher (0–1) excited vibronic state and suggests the formation of H-type cofacial π–π stacking between the PBI units.[20] Concentration-dependent CD measurements provide insight into the helical self-assembly of **DPPBI** in toluene. At a concentration of 10^{-3} mol L^{-1}, the CD spectra of **DPPBI** show a negative Cotton effect, followed by a positive Cotton effect at a higher wavelength, with the CD signal passing through zero near the

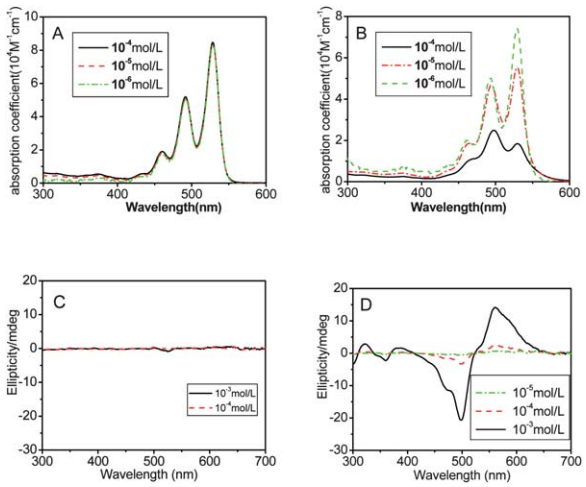

Fig. 2 Concentration-dependent UV-vis spectra of **SAPBI** (A) and **DPPBI** (B) in toluene at 20 °C and the concentration-dependent CD spectra of **SAPBI** (C) **DPPBI** (D) in toluene at 20 °C.

absorption maximum of **DPPBI**. As the concentration was reduced, the intensity of the signal continued to decrease until it reached the baseline at 10^{-5} mol L^{-1} (Fig. 3D). These results indicate the formation of helical superstructures at a high concentration.[21]

The large difference in the self-assembly behaviors of DPPBI and SAPBI suggests that a multivalent H-bonding interaction is crucial for the solution assembly. The hydrophilicity of the solvent has a pronounced effect on the self-assembly behavior of DPPBI, which shows a strong aggregation behavior in hydrophobic solvents, such as toluene and cyclohexane. However, aggregation does not occur in a hydrophilic solvent such as 1,4-dioxane, tetrahyrofuran, or dimethyl formamide (Figures S1 and S2 in the Supporting Information†). Hydrophilic solvents, which are usually hydrogen donors, interfere with the intermolecular hydrogen bonding between peptides.[22]

Thermal and mesomorphic properties

The thermotropic behavior of PBIs was investigated using a combination of differential scanning calorimetry (DSC), polarization optical microscopy, and X-ray diffraction (XRD) experiments. With a DSC scan from −60 to 200 °C, **SAPBI** only showed a phase transition at 150 °C, which is attributed to a phase transition from liquid crystalline mesophase to isotropic liquid state. The DSC analysis of **DPPBI** shows a phase behavior, where a liquid crystalline mesophase appeared at −27 °C and then disappeared at 181 °C to form an isotropic melt (Fig. 4A). The high isotropization temperature of **DPPBI** is the result of π–π stacking in the PBI columns and of hydrogen bond interactions of the amide groups, which reinforced the columnar organization. Columnar liquid crystals with a mesophase at room temperature, mesophase stability over a wide temperature range, and a single mesophase structure are desired for potential applications.[13]

As **DPPBI** cooled from their clearing temperatures to room temperature (20 °C), typical texture characteristics of the columnar phase were observed under a polarizing microscope (Fig. 3B). **DPPBI** exhibited a focal texture with straight linear defects, which is characteristic of ordered columnar mesophases.[23]

Fig. 4B shows the XRD profiles collected for the birefringent phase of PBIs at room temperature. The PBI birefringent phases were confirmed as a Colh phase through the assignment of the reflections. In the small-angle region, the XRD profile of **DPPBI** shows three reflection peaks corresponding to *d* spacings of 31.2, 18.1, and 15.2 Å, which are indexed in the sequence as (100), (110), and (200), respectively. In comparison, **DPPBI**, with dendritic peptide substituents, exhibited a smaller d100 value of 31.2 Å compared with **SAPBI**, which has swallow-tail amino acid substituents (d100 = 40.6 Å). In addition, the packing of the cores within the columns improved, as indicated by the sharp (001) reflection at $2\theta = 26.25°$. This reflection corresponds to an intermolecular distance of 3.4 Å between the aromatic cores of **DPPBI**, which is smaller than the spacing in the LC phase of **SAPBI** (3.5 Å), where the reflection is significantly broader. The XRD results show that **DPPBI** self-assembled into highly ordered columnar structures, in contrast to **SAPBI**, which is less ordered. Furthermore, the present study reports a new columnar PBI mesophase, in which hydrogen bond formation resulted in

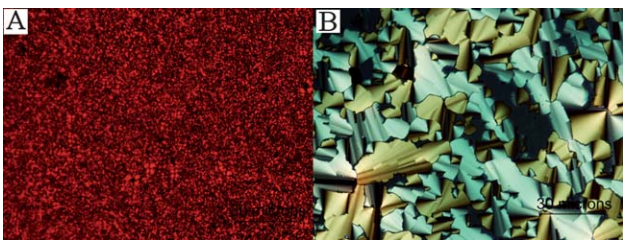

Fig. 3 (A) POMs of **SAPBI**, (B) POMs of **DPPBI** at 20 °C.

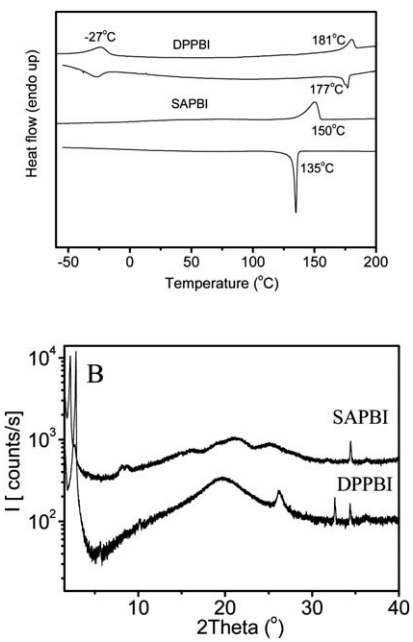

Fig. 4 (A) DSC of **SAPBI** and **DPPBI**, (B) XRD patterns of **SAPBI** and **DPPBI** at 20 °C.

the small inter-disk distance (3.4 Å) found in the columnar PBI liquid crystals.

The aggregation behavior of PBIs in the liquid crystalline mesophase was further investigated using temperature-dependent UV-Vis absorption spectroscopy on PBIs films (Fig. 5). From 170 (isotropic liquid state) to 20 °C (liquid crystalline state), **SAPBI** shows the J-aggregate, a considerably blue-shifted absorption band at around 400–500 nm, in addition to the aforementioned red-shifted band at 570 nm (Fig. 4, top).[24] By contrast, cooling from the clearing temperature of **DPPBI** to room temperature, the decreased absorption intensity of the 0–0 and increased absorption intensity of the 0–1 were observed, suggesting the formation of H-type cofacial π–π stacking between the **DPPBI** units. The formation of H-type cofacial π–π aggregation is ascribed to the hydrogen bonds between the **DPPBI** units in the liquid crystalline phases.

The presence of the hydrogen bonds in the liquid-crystalline phases of **DPPBI** was demonstrated by temperature-dependent Fourier transform infrared spectroscopic (FT-IR) studies (Fig. 6A). Cooling from 190 (isotropic state) to 20 °C (liquid crystalline state) resulted in a decline in the absorption intensities of the free amide groups at 1693 cm^{-1}. On the other hand, the absorption intensities of the hydrogen bonds of the amide groups at 1660 cm^{-1} increase. Furthermore, the N–H stretching frequency of DPPBI shifts from 3378 cm^{-1} (190 °C) to 3368 cm^{-1} (20 °C), indicating hydrogen bond formation in the mesophase. With the high selectivity and directionality of hydrogen bonds, the formation of the hydrogen bonds should contribute to the induction of the columnar liquid crystalline properties.

The higher helical order in the liquid crystal phase was further demonstrated by CD measurements. The CD spectra of **DPPBI** in the thin-film states show the same Cotton effect observed in a solution of **DPPBI** (Fig. 6B). The CD signal for the fresh film shows a weak intensity. However, the intensity increased after heating to 180 °C and then cooling to 20 °C. These results demonstrate the formation of helical superstructures in the liquid crystal phase.

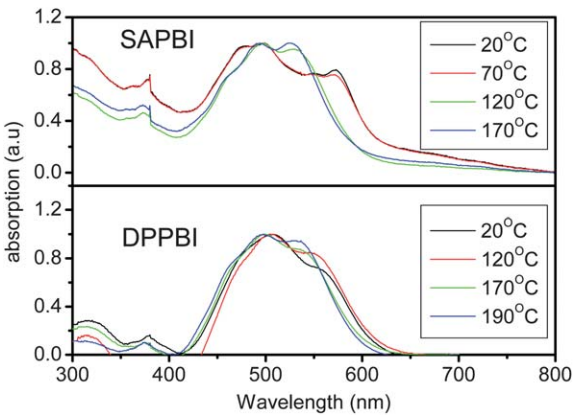

Fig. 5 Temperature dependent UV-vis absorption spectra of **SAPBI** film (top) and **DPPBI** film (bottom).

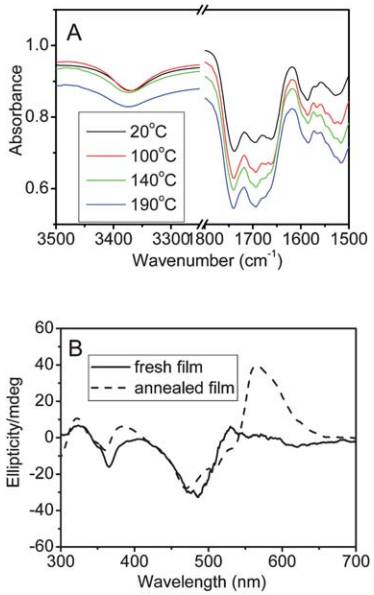

Fig. 6 (A) Temperature dependent FT-IR of **DPPBI** and (B) CD spectra of **DPPBI** in thin film states at 20 °C.

Conclusions

The present study succeeded in developing novel liquid crystal-based PBIs. The dendritic moieties, acting as *N*-substituents, induced the formation of a columnar liquid crystalline structure. The hydrogen bonds at the PBI peripheries resulted in the ordered columnar mesophases and small inter-disk distance (3.4 Å) in the columnar PBIs liquid crystalline structure. Meanwhile, the chiral peptides induced PBIs to assemble helical superstructures in the liquid crystalline mesophase. This property, along with the room temperature liquid crystalline structure and inherent optoelectronic properties of the PBIs core, makes dendritic peptide-substituted PBIs a promising material for use in optoelectronic devices.

Acknowledgements

This work was supported by the National Natural Science Foundation of China (Nos.20804012), the National Natural Science Foundation of Hebei Province (Nos. B2009000169), the Science Research Project of Department of Education of Hebei Province (Nos.2007413), the National Natural Science Foundation of Hebei University (Nos.2007105).

Notes and references

1 (*a*) J. Wu, W. Pisula and K. Müllen, *Chem. Rev.*, 2007, **107**, 718; (*b*) W. Pisula, A. Menon, M. Stepputat, I. Lieberwirth, U. Kolb, A. Tracz, H. Sirringhaus, T. Pakula and K. Müllen, *Adv. Mater.*, 2005, **17**, 684; (*c*) L. Schmidt, A. Fechtenkötter, E. Moons, R. H. Friend and J. D. MacKenzie, *Science*, 2001, **293**, 1119.

2 (*a*) A. M. van de Craats, N. Stutzmann, O. Bunk, M. M. Nielsen, M. Watson, K. Müllen, H. D. Chanzy, H. Sirringhaus and R. H. Friend, *Adv. Mater.*, 2003, **15**, 495; (*b*) J. Piris, M. G. Debije, N. Stutzmann, A. van de Craats, M. D. Watson, K. Müllen and J. M. Warman, *Adv. Mater.*, 2003, **15**, 1736.

3 A. M. van de Craats, J. M. Warman, A. Fechtenkötter, J. D. Brand, M. A. Harbison and K. Müllen, *Adv. Mater.*, 1999, **11**, 1469.

4 D. Adam, P. Schumacher, J. Simmerer, L. Haüsling, K. Siemensmeyer, K. H. Etzbach, H. Ringsdorf and D. Harrer, *Nature*, 1994, **371**, 141.
5 L. Brunsveld, E. W. Meijer, R. B. Prince and Jeffrey S. Moore, *J. Am. Chem. Soc.*, 2001, **123**, 7978.
6 J. Wu, M. D. Watson, L. Zhang, Z. Wang and K. Müllen, *J. Am. Chem. Soc.*, 2004, **126**, 177.
7 (*a*) B. Gómez-Lor, B. Alonso, A. Omenat and J. L. Serrano, *Chem. Commun.*, 2006, 5012; (*b*) E. M. García-Frutos, A. Omenat, J. Barberá, J. L. Serrano and B. Gómez-Lor, *J. Mater. Chem.*, 2011, **21**, 6831.
8 H. Engelkamp, S. Middlebeek and R. J. M. Nolte, *Science*, 1999, **284**, 785.
9 Z. An, J. Yu, B. Domercq, S. C. Jones, S. Barlow, B. Kippelen and S. R. Marder, *J. Mater. Chem.*, 2009, **19**, 6688–6698.
10 Z. An, J. Yu, S. C. Jones, S. Barlow, S. Yoo, B. Domercq, P. Prins, L. D. A. Siebbeles, B. Kippelen and S. R. Marder, *Adv. Mater.*, 2005, **17**, 2580.
11 (*a*) F. Würthner, *Chem. Commun.*, 2004, 1564–1579; (*b*) T. Kato, T. Yasuda, Y. Kamikawa and M. Yoshio, *Chem. Commun.*, 2009, 729.
12 (*a*) F. Würthner, C. Thalacker, S. Diele and C. Tschierske, *Chem.–Eur. J.*, 2001, **7**, 2245; (*b*) Z. Chen, U. Baumeister, C. Tschierske and F. Würthner, *Chem.–Eur. J.*, 2007, **13**, 450.
13 Y. Xu, S. Leng, C. Xue, R. Sun, J. Pan, J. Ford and S. Jin, *Angew. Chem., Int. Ed.*, 2007, **46**, 3896.
14 (*a*) A. Wicklein, A. Lang, M. Muth and M. Thelakkat, *J. Am. Chem. Soc.*, 2009, **131**, 14442; (*b*) A. Wicklein, P. Kohn, L. Ghazaryan, T. Thurn-Albrecht and M. Thelakkat, *Chem. Commun.*, 2010, **46**, 2328.
15 V. Dehm, Z. Chen, U. Baumeister, P. Prins, L. D. A. Siebbeles and F. Würthner, *Org. Lett.*, 2007, **9**, 1085.
16 B. Donnio, S. Buathong, I. Bury and D. Guillon, *Chem. Soc. Rev.*, 2007, **36**, 1495.
17 V. Percec, C. M. Mitchell, W. D. Cho, S. Uchida, M. Glodde, G. Ungar, X. Zeng, Y. Liu, V. S. K. Balagurusamy and P. A. Heiney, *J. Am. Chem. Soc.*, 2004, **126**, 6078.
18 (*a*) M. Nishii, T. Matsuoka, Y. Kamikawa and T. Kato, *Org. Biomol. Chem.*, 2005, **3**, 875; (*b*) Y. Kamikawa and T. Kato, *Org. Lett.*, 2006, **8**, 2463.
19 (*a*) R. Sun, C. Xue, M. Owak, R. M. Peetz and S. Jin, *Tetrahedron Lett.*, 2007, **48**, 6696; (*b*) C. Xue, R. Sun, R. Annab and D. Abadi, *Tetrahedron Lett.*, 2009, **50**, 853.
20 J. Wang, A. Kulago, W. R. Browne and B. L. Feringa, *J. Am. Chem. Soc.*, 2010, **132**, 4191.
21 J. H. K. Ky Hirschberg, L. Brunsveld, A. Ramzi, J. A. J. M. Vekemans, R. P. Sijbesma and E. W. Meijer, *Nature*, 2000, **407**, 167.
22 R. Matmour, I. De Cat, S. J. George, W. Adriaens, P. Leclere, P. H. H. Bomans, N. A. J. M. Sommerdijk, J. C. Gielen, P. C. M. Christianen, J. T. Heldens, J. C. M. van Hest, D. W. P. M. Lowik, S. De Feyter, E. W. Meijer and A. P. H. J. Schenning, *J. Am. Chem. Soc.*, 2008, **130**, 14576.
23 S. Laschat, A. Baro, N. Steinke, F. Giesselmann, C. Hgele, G. Scalia, R. Judele, E. Kapatsina, S. Sauer, A. Schreivogel and M. Tosoni, *Angew. Chem., Int. Ed.*, 2007, **46**, 4832.
24 S. Yagai, T. Seki, T. Karatsu, A. Kitamura and F. Würthner, *Angew. Chem., Int. Ed.*, 2008, **47**, 3367.

